

SUPPLEMENTARY MATERIALS

Altered muscle oxidative phenotype impairs exercise tolerance but does not improve after exercise training in multiple sclerosis

Jan Spaas^{1,2,3,}, Richie P. Goulding^{4,*}, Charly Keytsman^{1,2}, Lena Fonteyn^{1,2}, Jack van Horssen^{1,5}, Richard T. Jaspers⁴, Bert O. Eijnde^{1,2,**}, Rob C.I. Wüst^{4,**}*

¹ *University MS Center (UMSC) Hasselt – Pelt, Belgium.*

² *SMRC Sports Medical Research Center, BIOMED Biomedical Research Institute, Faculty of Medicine and Life Sciences, Hasselt University, Hasselt, Belgium.*

³ *Department of Movement and Sports Sciences, Faculty of Medicine and Health Sciences, Ghent University, Ghent, Belgium.*

⁴ *Laboratory for Myology, Faculty of Behavioural and Movement Sciences, Vrije Universiteit Amsterdam, Amsterdam Movement Sciences, Amsterdam, The Netherlands.*

⁵ *Department of Molecular Cell Biology and Immunology, Amsterdam Neuroscience, MS Center Amsterdam, Amsterdam University Medical Center, Location VUmc, Amsterdam, The Netherlands.*

* shared first author

** shared last author

Corresponding authors: Bert O. Eijnde (bert.opteijnde@uhasselt.be) and Rob C.I. Wüst (r.wust@vu.nl)

Supplementary Methods

Muscle strength

Following a 5-min standardized warm-up (cycle ergometer), maximal voluntary isometric muscle strength of the knee extensors of MS patients was measured using a System 3 (BiodexVR, ENRAF-NONIUS, NY). Knee angle was set at 90°. Maximal contractions lasted 4 s and were repeated twice (30 s rest interval). The highest isometric extension torque (Nm) was used for data analysis. Baseline results were used to classify the legs of each MS patient as the weakest or strongest leg. Biopsies were taken from the weakest leg [1].

Exercise capacity

Peak power output was determined as the highest stage completed during the test. Peak values for $\dot{V}O_2$ ($\dot{V}O_{2peak}$), carbon dioxide output ($\dot{V}CO_{2peak}$), heart rate (HR_{peak}), O_2 pulse (i.e., $\dot{V}O_{2peak}/HR_{peak}$; O_2 pulse_{peak}), ventilation ($\dot{V}E_{peak}$), respiratory exchange ratio (RER_{peak}), ventilatory equivalents for O_2 (i.e., $\dot{V}E_{peak}/\dot{V}O_{2peak}$) and CO_2 (i.e., $\dot{V}E_{peak}/\dot{V}CO_{2peak}$), end-tidal O_2 ($PETO_{2peak}$) and CO_2 ($PETCO_{2peak}$) tensions, tidal volume (V_{Tpeak}) and breathing frequency (B_{Fpeak}) were determined as the highest 20 second averages attained during the tests. The gas exchange threshold (GET) was determined as a non-invasive estimate of the lactate threshold via visual inspection of the data using a cluster of predefined criteria, including: a disproportionate increase in $\dot{V}CO_2$ relative to $\dot{V}O_2$; an increase in $\dot{V}E$ relative to $\dot{V}O_2$ ($\dot{V}E/\dot{V}O_2$) without an increase in $\dot{V}E$ relative to $\dot{V}CO_2$ ($\dot{V}E/\dot{V}CO_2$); and an increase in end-tidal O_2 tension ($PETO_2$) without decreasing end-tidal CO_2 tension ($PETCO_2$). The respiratory compensation point (RCP) was determined as the $\dot{V}O_2$ at which $PETCO_2$ began to fall after a period of isocapnic buffering (i.e., stable $PETCO_2$), corroborated by the second and first breakpoints in the $\dot{V}E$ - and $\dot{V}E/\dot{V}CO_2$ relationships, respectively. The 'gain' of the $\dot{V}O_2$ response was calculated as the slope of the linear relationship

between $\dot{V}O_2$ and power output, as previously described [2]. Briefly, data from the start of the test before the linear rise in $\dot{V}O_2$ had begun, as well as any non-linearities in the $\dot{V}O_2$ response towards the end of the test either due to a slow component-like phenomenon or a plateau, were excluded. The slope of the $\dot{V}E$ - $\dot{V}CO_2$ relationship was calculated in a similar fashion, following exclusion of non-linearities at the very onset of test and data from above the RCP [3]. The $\dot{V}O_2$ -HR slope was calculated from test onset until end-exercise.

Muscle fiber type composition and fiber size

Sections (10 μ m) were washed in phosphate-buffered saline (PBS) with 0.05% Triton-X100 and blocked with 10% goat serum (60 min). Next, primary mouse anti-myosin heavy chain monoclonal antibodies BA-F8 (to visualise type I fibers, IgG2b, 1:100), SC-71 (type IIa fibers, IgG1, 1:100) and 6H1 (type IIx fibers, IgM, 1:100) from the Developmental Studies Hybridoma Bank (DSHB, University of Iowa) and rabbit anti-laminin polyclonal antibody PA1-16730 (IgG, 1:200, Invitrogen) were applied for 120 min in PBS with 0.05% Triton-X100 and 10% goat serum. Sections were washed (3 \times 5 min) and exposed to complementary secondary goat anti-mouse AF 350 (IgG2b), AF 488 (IgG1), AF 555 (IgM) and goat anti-rabbit AF 647 (IgG) antibodies (Invitrogen), each diluted 1:250 in PBS with 0.05% Triton-X100 and 10% goat serum. Finally, sections were washed in PBS and mounted with fluorescent mounting medium.

A small amount of hybrid fibers expressing both the MyHC type I and IIa isoforms was found in 7/16 patients and 5/15 controls, however, these were excluded from the analysis.

Muscle SDH activity

Immediately after cutting, sections (10 μ m) were air-dried for 15 min and then immersed in a pre-heated (37°C) solution containing sodium phosphate buffer (37 mM, pH 7.6), sodium succinate (74 mM), sodium azide (5 mM) and tetranitroblue tetrazolium (TNBT, 0.4 mM, Sigma) for 20 min in the

dark. The succinate dehydrogenase enzyme oxidizes succinate to fumarate, resulting in a blue colour. The reaction was stopped by brief HCl (10 mM) exposure before sections were mounted with glycerine/gelatine [4, 5]. Stained sections were stored at 4°C and imaged within 10 days using a DMRB microscope (Leica) with calibrated grey filters. The spatially averaged SDH activity of muscle fibers, including subsarcolemmal mitochondria, was obtained from 660 nm absorbance measurements using ImageJ (NIH), expressed as ΔA_{660} per μm tissue thickness per second of staining time ($\Delta A_{660} \cdot \mu\text{m}^{-1} \cdot \text{s}^{-1}$).

Muscle capillarity

Sections (10 μm) were washed (PBS) and exposed to primary antibodies overnight at 4°C (CD31: mouse monoclonal, 1:100, DAKO M0823 clone JC70A; laminin: rabbit polyclonal, 1:200, Sigma L9393), diluted in PBS containing 1% bovine serum albumin (BSA). The next day, sections were washed (3 \times 5 min, PBS) and incubated with secondary goat anti-mouse (AF 488, 1:250) and goat anti-rabbit (AF 555, 1:250) antibodies (Invitrogen), diluted in PBS containing 1% BSA. Finally, sections were stained with DAPI, washed in PBS, and mounted with fluorescent mounting medium.

Protein concentrations

Snap-frozen muscle tissue was homogenised with a QIAGEN TissueRuptor on ice in RIPA buffer (50 mM Tris pH 8.0, 150 mM NaCl, 0.5% sodium deoxycholate, 0.1% SDS, 1% Triton-X100, and freshly added protease/phosphatase inhibitors [Roche]). Samples were centrifuged (15 min, 12500 \times g, 4°C) and supernatant was stored at -80°C. Protein content was measured with Pierce™ BCA Protein Assay Kit (Thermo Fisher) according to manufacturer's instructions and read at 570 nm wavelength.

For detection of PGC-1 α protein levels, the loading buffer solution was prepared as follows: 3.55 mL milliQ water, 1.25 mL 0.5 M Tris-HCl pH 6.8, 2.5 mL glycerol, 2 mL 10% SDS, 0.1 mL 1% bromophenol blue. Right before sample preparation, β -mercaptoethanol was added (5%). Protein samples (10 μg)

were diluted in loading buffer, heated for 4 min at 95°C, separated in polyacrylamide gels and transferred to PVDF membranes (90 min, 350 mA). Membranes were blocked in Tris-buffered saline with 0.1% Tween20 (TBS-T) containing 5% milk powder (60 min) and incubated overnight at 4°C with primary antibodies against PGC-1 α (ab191838, rabbit polyclonal, 1:2000, Abcam) diluted in 5% milk. Secondary HRP-conjugated swine anti-rabbit antibodies (1:2500, in 5% milk) were then applied for 90 min at room temperature. Blots were developed in an Amersham™ Imager 680 using chemiluminescent detection (Pierce™ ECL Plus Western Blotting Substrate, Thermo Fisher). Between different steps, membranes were washed 3 \times 5 min with TBS-T. Blots were stripped and stained for β -actin (1:2500, Santa Cruz) as loading control. All blots were run in parallel on the same day with identical exposure time and imager settings. Protein bands (a.u.) were quantified with ImageJ (NIH) by a blinded assessor. Samples from MS patients and controls were loaded alternately on every blot, with pre/post samples from patients engaging in the exercise intervention loaded in adjacent lanes.

To measure protein levels of the five mitochondrial OXPHOS complexes, samples (10 μ g) were diluted in 4 x Laemmli buffer (Bio-Rad 1610747) containing Dithiothreitol (DTT). Samples were separated in polyacrylamide gels and transferred to PVDF membranes (60 min, 80 V). Hereafter, membranes were incubated in Ponceau S (Sigma 81462) to stain all membrane proteins. Membranes were washed (TBS-T), followed by a blocking step (TBS-T containing 2% ECL Prime blocking agent [RPN418], 60 min) and overnight incubation (4°C) with primary antibodies (i.e. OXPHOS cocktail, ab110413, mouse monoclonal, 1:1000 in blocking buffer, Abcam). Secondary HRP-conjugated goat anti-mouse antibodies (1:2500) were then applied for 60 min at room temperature. Blots were developed in a LAS500 imager using chemiluminescent detection (Amersham, Cytiva RPN 2235). Between different steps, membranes were washed 3 \times 5 min with TBS-T. Protein bands of every mitochondrial complex were quantified with ImageJ (NIH) by a blinded assessor, and normalized to Ponceau S staining intensity. Samples from MS patients and controls were loaded alternately on every blot, with pre/post samples from patients engaging in the exercise intervention loaded in adjacent lanes. Data are expressed as % relative to control subjects. In addition, we quantified the overall average

mitochondrial OXPHOS protein content as the sum of all five complexes (after data were expressed relative to controls).

Gene expression analysis

Snap-frozen muscle samples were lysed in 500 μ L Qiazol buffer (Qiagen) and mixed with 100 μ L chloroform. Following centrifugation, the RNA phase was diluted in 250 μ L isopropanol and incubated overnight at -20°C . The next day, samples were centrifuged and the RNA pellet was resuspended in 75% and 100% ethanol solutions. Finally, the RNA pellet was air-dried and, diluted in RNase-free water and the RNA yield and purity were measured with a NanoDrop spectrophotometer (Thermo Fisher).

Next, cDNA with a final concentration of 5 ng/ μ L was synthesized using qScript™ cDNA SuperMix (Quantabio). Real-time quantitative PCR (qPCR) was conducted on a QuantStudio 3 system using Fast SYBR™ Green Master Mix (Applied Biosystems).

References Supplementary Methods

1. Keytsman, C., et al., *Impact of high-intensity concurrent training on cardiovascular risk factors in persons with multiple sclerosis—pilot study*. Disability and Rehabilitation, 2017: p. 1-6.
2. Goulding, R.P., D.M. Roche, and S. Marwood, *Prior exercise speeds pulmonary oxygen uptake kinetics and increases critical power during supine but not upright cycling*. Experimental physiology, 2017. **102**(9): p. 1158-1176.
3. Gavotto, A., et al., *The $\dot{V}_e/\dot{V}_{\text{CO}_2}$ slope: a useful tool to evaluate the physiological status of children with congenital heart disease*. Journal of Applied Physiology, 2020. **129**(5): p. 1102-1110.

4. van der Zwaard, S., et al., *Adaptations in muscle oxidative capacity, fiber size, and oxygen supply capacity after repeated-sprint training in hypoxia combined with chronic hypoxic exposure*. *Journal of Applied Physiology*, 2018. **124**(6): p. 1403-1412.
5. Bekedam, M.A., et al., *Maximum rate of oxygen consumption related to succinate dehydrogenase activity in skeletal muscle fibres of chronic heart failure patients and controls*. *Clinical physiology and functional imaging*, 2003. **23**(6): p. 337-343.

Supplementary Discussion

Supplementary Discussion 1

Among a host of measures related to aerobic function, we have presented data for the gold-standard for assessing whole-body aerobic capacity in humans, namely $\dot{V}O_{2\text{peak}}$. Indeed, this variable is highly clinically relevant, reflecting one of the best predictors of all-cause mortality across both health and disease [1, 2]. Moreover, we present data regarding leg muscle strength (determined via maximal voluntary isometric contractions), which is similarly predictive of clinical outcomes and all-cause mortality across various populations [3, 4]. Hence, whilst walking capacity is a functional outcome of interest, walking capacity is itself determined by a combination of both muscle strength and aerobic capacity. This latter notion is supported by studies that have shown strong relationships between 6 minute walk test performance and both muscle strength [5] and $\dot{V}O_{2\text{peak}}$ [6]. The contribution of muscle strength and muscle oxidative capacity have also been shown to be related to walking capacity in MS patients [7, 8].

Supplementary Discussion 2

Short-duration high-intensity interval training (HIIT) such as that employed in the present study has been shown to upregulate a host of peripheral processes involved in oxygen utilization, such as mitochondrial biogenesis [9], promotion of skeletal muscle mitochondrial content [10-12], function [13, 14], and capillarization [15]. Whilst the capacity for mitochondrial oxidative phosphorylation exceeds the maximal capacity for oxygen delivery, it is now widely accepted that muscle oxygen consumption represents an integrated control system where flux control is shared across each step in the pathway. Hence, alterations in the capacities of any step along the pathway will alter the maximal flux (i.e., $\dot{V}O_{2\text{peak}}$) [16, 17]. This concept is elegantly illustrated by Cardinale *et al.* [18], who

demonstrated that mitochondrial excess capacity serves to maintain a low P_{50} for O_2 , which enhances O_2 diffusion from the microcirculation to mitochondria during exercise. Therefore, alterations in mitochondrial function following training contribute to increased diffusive O_2 flux and thus maximal O_2 extraction and $\dot{V}O_{2peak}$. Hence, whilst central adaptations do occur following short-duration HIIT [19], it is indubitable that peripheral adaptations also occur and contribute to changes in $\dot{V}O_{2peak}$ following training. That these adaptations did not occur following our 12 week HIIT program in MS thus further highlights the lack of plasticity of skeletal muscle in this population.

Supplementary Discussion 3

Additional references: [20, 21]

References Supplementary Discussion

1. Myers, J., et al., *Fitness versus physical activity patterns in predicting mortality in men*. The American journal of medicine, 2004. **117**(12): p. 912-918.
2. Myers, J., et al., *Exercise capacity and mortality among men referred for exercise testing*. New England journal of medicine, 2002. **346**(11): p. 793-801.
3. Li, R., et al., *Associations of muscle mass and strength with all-cause mortality among US older adults*. Medicine and science in sports and exercise, 2018. **50**(3): p. 458.
4. Metter, E.J., et al., *Skeletal muscle strength as a predictor of all-cause mortality in healthy men*. The Journals of Gerontology Series A: Biological Sciences and Medical Sciences, 2002. **57**(10): p. B359-B365.
5. Pradon, D., et al., *Relationship between lower limb muscle strength and 6-minute walk test performance in stroke patients*. Journal of Rehabilitation Medicine, 2013. **45**(1): p. 105-108.

6. Ross, R.M., et al., *The six minute walk test accurately estimates mean peak oxygen uptake.* BMC pulmonary medicine, 2010. **10**(1): p. 1-9.
7. Van Geel, F., et al., *Is maximal muscle strength and fatigability of three lower limb muscle groups associated with walking capacity and fatigability in multiple sclerosis? An exploratory study.* Multiple Sclerosis and Related Disorders, 2021. **50**: p. 102841.
8. Hansen, D., et al., *Is walking capacity in subjects with multiple sclerosis primarily related to muscle oxidative capacity or maximal muscle strength? A pilot study.* Mult Scler Int, 2014. **2014**: p. 759030.
9. Little, J.P., et al., *An acute bout of high-intensity interval training increases the nuclear abundance of PGC-1 α and activates mitochondrial biogenesis in human skeletal muscle.* American Journal of Physiology-Regulatory, Integrative and Comparative Physiology, 2011.
10. Gibala, M.J., et al., *Short-term sprint interval versus traditional endurance training: similar initial adaptations in human skeletal muscle and exercise performance.* The Journal of physiology, 2006. **575**(3): p. 901-911.
11. Ma, J.K., et al., *Extremely low-volume, high-intensity interval training improves exercise capacity and increases mitochondrial protein content in human skeletal muscle.* Open Journal of Molecular and Integrative Physiology, 2013. **2013**.
12. Burgomaster, K.A., et al., *Six sessions of sprint interval training increases muscle oxidative potential and cycle endurance capacity in humans.* Journal of applied physiology, 2005.
13. Larsen, F.J., et al., *Mitochondrial oxygen affinity increases after sprint interval training and is related to the improvement in peak oxygen uptake.* Acta physiologica, 2020. **229**(3): p. e13463.
14. Vincent, G., et al., *Changes in mitochondrial function and mitochondria associated protein expression in response to 2-weeks of high intensity interval training.* Frontiers in physiology, 2015: p. 51.

15. Scribbans, T.D., et al., *Fibre-specific responses to endurance and low volume high intensity interval training: striking similarities in acute and chronic adaptation*. PloS one, 2014. **9**(6): p. e98119.
16. Lindstedt, S.L., R.G. Thomas, and D.E. Leith, *Does peak inspiratory flow contribute to setting $\dot{V}O_{2max}$? A test of symmorphosis*. Respiration physiology, 1994. **95**(1): p. 109-118.
17. Lindstedt, S.L. and K. Conley, *Human aerobic performance: too much ado about limits to VO_2* . Journal of Experimental Biology, 2001. **204**(18): p. 3195-3199.
18. Cardinale, D.A., et al., *Muscle mass and inspired oxygen influence oxygen extraction at maximal exercise: role of mitochondrial oxygen affinity*. Acta Physiologica, 2019. **225**(1): p. e13110.
19. Mandić, M., et al., *Improvements in Maximal Oxygen Uptake after Sprint Interval Training Coincide with Increases in Central Hemodynamic Factors*. Medicine and Science in Sports and Exercise, 2022.
20. van den Berg-Emons, R.J., et al., *Validation of the Physical Activity Scale for individuals with physical disabilities*. Archives of physical medicine and rehabilitation, 2011. **92**(6): p. 923-928.
21. van der Ploeg, H.P., et al., *The Physical Activity Scale for Individuals with Physical Disabilities: test-retest reliability and comparison with an accelerometer*. Journal of Physical Activity and Health, 2007. **4**(1): p. 96-100.

Supplementary Table 1. Primer sequences.

Gene	Full name	Fw primer sequence	Rv primer sequence
<i>COX4I1</i>	Cytochrome C Oxidase Subunit 4I1	CGAGCAATTTCCACCTCTGT	GGTCACGCCGATCCATATAA
<i>CS</i>	Citrate Synthase	CCTGCCTAATGACCCCATGTT	CATAATACTGGAGCAGCACCCC
<i>PPARA</i>	Peroxisome Proliferator-Activated Receptor Alpha	GTGGCTGCTATCATTGCTGTG	CACATGTAAATACCCTCCTGCAT
<i>PPARG</i>	Peroxisome Proliferator-Activated Receptor Gamma	GATGTCTCATAATGCCATCAGGTT	GGATTGAGCTGGTGGATCACT
<i>PPARGC1A</i>	Peroxisome Proliferator-Activated Receptor Gamma Coactivator 1-Alpha	TTCCACCAAGAGCAAGTAT	CGCTGTCCCATGAGGTATT
<i>SDHB</i>	Succinate Dehydrogenase Complex, Subunit B, Iron Sulfur	TAGCTTGACCCGAAGGATTGACACC	CGCTCTTCTATGGACTGCAGATACTGC
<i>TFAM</i>	Transcription Factor A, Mitochondrial	TCCGCCCTATAAGCATCTTG	CCGAGGTGGTTTTTCATCTGT
Housekeeping genes			
<i>RPL13A</i>	Ribosomal Protein L13a	AAGTTGAAGTACCTGGCTTTCC	GCCGTCAAACACCTTGAGAC
<i>GAPDH</i>	Glyceraldehyde-3-Phosphate Dehydrogenase	TCAAGGCTGAGAACGGGAAG	CGCCCCACTTGATTTGGAG

List of primers used for gene expression analysis (qPCR) of human muscle tissue. The housekeeping genes were chosen based on stability analysis (geNorm software).

Supplementary Table 2. Cardiopulmonary exercise test variables in MS patients and healthy controls

CPET variables	MS (n=19)	Controls (n=16)	P value
Peak power output (W)	134 ± 65	178 ± 58	0.033 *
Test duration (min)	9.6 ± 4.3	13.9 ± 3.7	0.002 **
$\dot{V}O_{2peak}$ (mL·min ⁻¹)	1778 ± 729	2431 ± 664	0.010 *
$\dot{V}O_{2peak}$ (mL·min ⁻¹ ·kg ⁻¹)	25.0 ± 8.5	35.7 ± 6.4	<0.001 **
Gain of $\dot{V}O_2$ vs. power output (mL·min ⁻¹ ·W ⁻¹)	9.5 ± 1.7	10.7 ± 1.1	0.013 *
GET (mL·min ⁻¹)	1042 ± 398	1337 ± 196	0.011 *
GET (% of $\dot{V}O_{2peak}$)	58.3 ± 8.4	57.1 ± 9.7	0.707
RCP (mL·min ⁻¹)	1507 ± 635	1967 ± 507	0.027 *
RCP (% of $\dot{V}O_{2peak}$)	83.0 ± 9.8	82.4 ± 12.0	0.870
HR _{peak} (beats·min ⁻¹)	155 ± 21	171 ± 15	0.014 *
$\dot{V}O_2$ -HR slope (beats·mL ⁻¹ ·min ⁻¹)	0.065 ± 0.027	0.055 ± 0.018	0.221
$\dot{V}E$ - $\dot{V}CO_2$ slope	33.3 ± 5.4	37.1 ± 7.4	0.084
$\dot{V}CO_{2peak}$ (mL·min ⁻¹)	2198 ± 890	2845 ± 777	0.030 *
O ₂ pulse _{peak} (mL·heartbeats ⁻¹)	11.4 ± 4.3	14.2 ± 3.7	0.043 *
RER _{peak}	1.25 ± 0.11	1.18 ± 0.06	0.049 *
$\dot{V}E_{peak}$ (L·min ⁻¹)	72.5 ± 27.3	90.7 ± 31.6	0.080
$\dot{V}E\%MVV$ (% predicted)	59.3 ± 16.4	72.7 ± 12.5	0.016 *
$\dot{V}E/\dot{V}O_{2peak}$	41.4 ± 5.8	37.0 ± 4.8	0.022 *
$\dot{V}E/\dot{V}CO_{2peak}$	33.3 ± 4.2	31.7 ± 5.2	0.332
PETCO _{2peak} (mmHg)	4.6 ± 0.6	5.0 ± 0.8	0.168
PETO _{2peak} (mmHg)	15.9 ± 0.6	15.6 ± 0.7	0.280
V _{Tpeak} (L)	2.1 ± 0.8	2.4 ± 0.8	0.340
B _{Fpeak} (breaths·min ⁻¹)	33.9 ± 10.7	39.7 ± 9.4	0.101

B_{Fpeak}, peak breathing frequency; GET, gas exchange threshold; HR_{peak}, peak heart rate; O₂ pulse_{peak}, peak oxygen pulse; PETCO_{2peak}, peak end-tidal CO₂ tension; PETO_{2peak}, peak end-tidal O₂ tension; RCP, respiratory compensation point; RER_{peak}, peak respiratory exchange ratio; $\dot{V}E/\dot{V}CO_2$, slope of the relationship between ventilation and carbon dioxide output; $\dot{V}E/\dot{V}CO_{2peak}$, peak ventilatory equivalent for CO₂; $\dot{V}E/\dot{V}O_{2peak}$, peak ventilatory equivalent for O₂; $\dot{V}E_{peak}$, peak minute ventilation; $\dot{V}E\%MVV$, $\dot{V}E_{peak}$ as a proportion of predicted maximal voluntary ventilation; $\dot{V}O_2$ -HR slope, slope of the relationship between oxygen consumption and heart rate; $\dot{V}CO_{2peak}$, peak carbon dioxide output; $\dot{V}O_{2peak}$, peak oxygen uptake; V_{Tpeak}, peak tidal volume. * indicates P < 0.05; ** indicates P < 0.01.

Supplementary Table 3. Variables derived from cardiopulmonary exercise testing, separated by sex.

CPET variables	Female		Male		P values		
	MS (n = 11)	HC (n = 10)	MS (n = 8)	HC (n = 6)	Gender × disease	Gender	Disease
Peak power output (W)	110 ± 48	147 ± 44	163 ± 74	231 ± 37	0.3730	<0.001 **	0.004 **
Test duration (min)	9.4 ± 4.0	13.7 ± 4.4	9.9 ± 5.0	14.4 ± 2.4	0.9310	0.638	0.005 **
$\dot{V}O_{2peak}$ (mL·min ⁻¹)	1401 ± 339	2025 ± 372	2297 ± 779	3107 ± 441	0.6013	<0.001 **	<0.001 **
$\dot{V}O_{2peak}$ (mL·min ⁻¹ ·kg ⁻¹)	21.6 ± 4.6	34.3 ± 6.3	29.6 ± 10.7	37.9 ± 6.4	0.3847	0.028 *	<0.001 **
Gain of $\dot{V}O_2$ vs. power output (mL·min ⁻¹ ·W ⁻¹)	9.0 ± 1.9	10.3 ± 1.0	10.3 ± 0.8	11.6 ± 0.6	0.9926	0.011 *	0.009 **
GET (mL·min ⁻¹)	817 ± 254	1248 ± 166	1395 ± 321	1486 ± 152	0.0487 *	<0.001 **	0.004 **
GET (% of $\dot{V}O_{2peak}$)	59.0 ± 9.4	62.5 ± 8.0	57.3 ± 7.4	48.1 ± 3.1	0.0286 *	0.007 **	0.313
RCP (mL·min ⁻¹)	1196 ± 429	1785 ± 331	1996 ± 616	2272 ± 620	0.3702	0.001 **	0.018 *
RCP (% of $\dot{V}O_{2peak}$)	84.5 ± 10.3	88.4 ± 6.0	80.7 ± 9.4	72.5 ± 13.3	0.0880	0.007 **	0.528
HR _{peak} (beats·min ⁻¹)	155 ± 18	170 ± 15	155 ± 25	172 ± 15	0.9356	0.924	0.019 *
$\dot{V}O_2$ -HR slope (beats·mL ⁻¹ ·min ⁻¹)	0.080 ± 0.026	0.064 ± 0.016	0.044 ± 0.009	0.040 ± 0.009	0.3496	<0.001 **	0.114
VE-VCO ₂ slope	33.3 ± 5.2	39.0 ± 8.2	33.2 ± 6.1	34.0 ± 4.9	0.2703	0.248	0.152
$\dot{V}CO_{2peak}$ (mL·min ⁻¹)	1778 ± 502	2377 ± 502	2777 ± 1009	3626 ± 433	0.5799	<0.001 **	0.003 **
O ₂ pulse _{peak} (mL·heartbeat ⁻¹)	9.1 ± 2.9	11.9 ± 1.9	14.5 ± 3.9	18.1 ± 2.2	0.6702	<0.001 **	0.003 **
RER _{peak}	1.28 ± 0.10	1.19 ± 0.07	1.20 ± 0.10	1.17 ± 0.03	0.2851	0.083	0.062
$\dot{V}E_{peak}$ (L·min ⁻¹)	60.2 ± 20.7	71.5 ± 20.1	89.4 ± 27.2	119.6 ± 21.8	0.2379	<0.001 **	0.013 *
$\dot{V}E\%MVV$ (% predicted)	56.2 ± 13.3	67.1 ± 13.5	63.7 ± 20.1	81.0 ± 8.6	0.5351	0.046 *	0.010 *
$\dot{V}E/\dot{V}O_{2peak}$	43.0 ± 5.5	36.2 ± 5.4	39.2 ± 5.7	38.4 ± 3.5	0.1088	0.690	0.046
$\dot{V}E/\dot{V}CO_{2peak}$	33.7 ± 4.8	30.5 ± 5.0	32.7 ± 3.4	33.8 ± 5.4	0.1902	0.478	0.516
PETCO _{2peak} (mmHg)	4.5 ± 0.7	5.1 ± 0.9	4.7 ± 0.6	4.7 ± 0.6	0.2728	0.741	0.271
PETO _{2peak} (mmHg)	16.1 ± 0.6	15.5 ± 0.8	15.6 ± 0.7	15.7 ± 0.5	0.1312	0.613	0.335
V _{Tpeak} (L)	1.7 ± 0.6	1.9 ± 0.4	2.7 ± 0.6	3.1 ± 0.5	0.5744	<0.001 **	0.093
B _{Fpeak} (breaths·min ⁻¹)	33.9 ± 12.8	40.6 ± 11.2	33.9 ± 7.7	38.2 ± 5.7	0.7464	0.738	0.139

B_{Fpeak}, peak breathing frequency; GET, gas exchange threshold; HR_{peak}, peak heart rate; O₂ pulse_{peak}, peak oxygen pulse; PETCO_{2peak}, peak end-tidal CO₂ tension; PETO_{2peak}, peak end-tidal O₂ tension; RCP, respiratory compensation point; RER_{peak}, peak respiratory exchange ratio; $\dot{V}E/\dot{V}CO_2$, slope of the relationship between ventilation and carbon dioxide output; $\dot{V}E/\dot{V}CO_{2peak}$, peak ventilatory equivalent for CO₂; $\dot{V}E/\dot{V}O_{2peak}$, peak ventilatory equivalent for O₂; $\dot{V}E_{peak}$, peak minute ventilation; $\dot{V}E\%MVV$, $\dot{V}E_{peak}$ as a proportion of predicted maximal voluntary ventilation; $\dot{V}O_2$ -HR slope, slope of the relationship between oxygen consumption and heart rate; $\dot{V}CO_{2peak}$, peak carbon dioxide output; $\dot{V}O_{2peak}$, peak oxygen uptake; V_{Tpeak}, peak tidal volume. * indicates P < 0.05; ** indicates P < 0.01.

Supplementary Table 4. Cardiopulmonary exercise test variables before and after exercise training in MS patients

CPET variables	MS pre training (n = 8)	MS post training (n = 8)	P value
Peak power output (W)	169 ± 71	193 ± 85	0.008 **
Test duration (min)	11.5 ± 3.6	13.3 ± 4.3	0.004 **
$\dot{V}O_{2peak}$ (mL·min ⁻¹)	2156 ± 882	2594 ± 1068	0.001 **
$\dot{V}O_{2peak}$ (mL·min ⁻¹ ·kg ⁻¹)	30.2 ± 9.6	37.1 ± 11.8	0.001 **
Gain of $\dot{V}O_2$ vs. power output (mL·min ⁻¹ ·W ⁻¹)	9.5 ± 2.0	10.4 ± 2.0	0.079
GET (mL·min ⁻¹)	1232 ± 464	1467 ± 601	0.048 *
GET (% of $\dot{V}O_{2peak}$)	58.0 ± 6.1	57.9 ± 8.6	0.978
RCP (mL·min ⁻¹)	1839 ± 793	2221 ± 967	0.008 **
RCP (% of $\dot{V}O_{2peak}$)	84.6 ± 6.5	85.3 ± 6.8	0.855
HR _{peak} (beats·min ⁻¹)	165 ± 14	164 ± 20	0.678
$\dot{V}O_2$ -HR slope (beats·mL ⁻¹ ·min ⁻¹)	0.055 ± 0.029	0.067 ± 0.034	0.009 **
$\dot{V}E$ - $\dot{V}CO_2$ slope	35.7 ± 4.9	30.3 ± 3.3	0.005 **
$\dot{V}CO_{2peak}$ (mL·min ⁻¹)	2705 ± 1008	2891 ± 878	0.157
O ₂ pulse _{peak} (mL·heartbeat ⁻¹)	13.1 ± 5.3	15.8 ± 6.2	<0.001 **
RER _{peak}	1.28 ± 0.11	1.17 ± 0.17	0.077
$\dot{V}E_{peak}$ (L·min ⁻¹)	86.3 ± 29.5	105.1 ± 37.4	0.003 **
$\dot{V}E\%MVV$ (% predicted)	59.9 ± 28.4	72.4 ± 33.6	0.002 **
$\dot{V}E/\dot{V}O_{2peak}$	28.3 ± 8.0	41.7 ± 5.7	0.017 *
$\dot{V}E/\dot{V}CO_{2peak}$	30.2 ± 4.0	35.8 ± 3.9	0.038 *
PETCO _{2peak} (mmHg)	4.8 ± 0.6	4.4 ± 0.4	0.145
PETO _{2peak} (mmHg)	15.8 ± 0.6	15.7 ± 0.4	0.621
V _{Tpeak} (L)	2.3 ± 0.8	2.3 ± 0.7	0.631
B _{Fpeak} (breaths·min ⁻¹)	38.9 ± 5.6	47.4 ± 7.9	0.022 *

B_{Fpeak}, peak breathing frequency; GET, gas exchange threshold; HR_{peak}, peak heart rate; O₂ pulse_{peak}, peak oxygen pulse; PETCO_{2peak}, peak end-tidal CO₂ tension; PETO_{2peak}, peak end-tidal O₂ tension; RCP, respiratory compensation point; RER_{peak}, peak respiratory exchange ratio; $\dot{V}E/\dot{V}CO_2$, slope of the relationship between ventilation and carbon dioxide output; $\dot{V}E/\dot{V}CO_{2peak}$, peak ventilatory equivalent for CO₂; $\dot{V}E/\dot{V}O_{2peak}$, peak ventilatory equivalent for O₂; $\dot{V}E_{peak}$, peak minute ventilation; $\dot{V}E\%MVV$, $\dot{V}E_{peak}$ as a proportion of predicted maximal voluntary ventilation; $\dot{V}O_2$ -HR slope, slope of the relationship between oxygen consumption and heart rate; $\dot{V}CO_{2peak}$, peak carbon dioxide output; $\dot{V}O_{2peak}$, peak oxygen uptake; V_{Tpeak}, peak tidal volume. * indicates P < 0.05; ** indicates P < 0.01.

Supplementary Table 5. Baseline muscle fiber SDH activity in healthy controls, all MS patients, and the MS training subgroup.

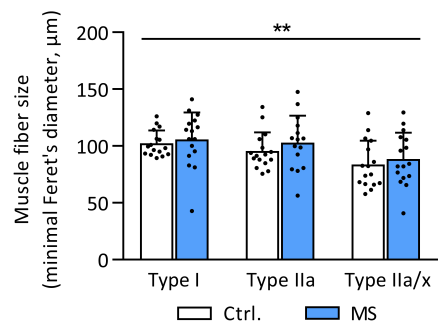
	Controls (n = 15)	MS (n = 15)	MS intervention study (n = 5)
Type I fiber SDH activity	1.81 ± 0.39	1.39 ± 0.27	1.45 ± 0.23
Type IIa fiber SDH activity	1.45 ± 0.29	1.09 ± 0.24	1.24 ± 0.17
Type IIa/x fiber SDH activity	1.10 ± 0.16	0.99 ± 0.21	1.12 ± 0.15
Weighted SDH activity	1.51 ± 0.31	1.16 ± 0.22	1.32 ± 0.19

Muscle fiber SDH activity for healthy control subjects and MS patients (whole group and subjects that were enrolled in the training intervention). SDH activity is expressed as $\Delta A_{660} \cdot \mu\text{m}^{-1} \cdot \text{s}^{-1} \times 10^{-5}$.

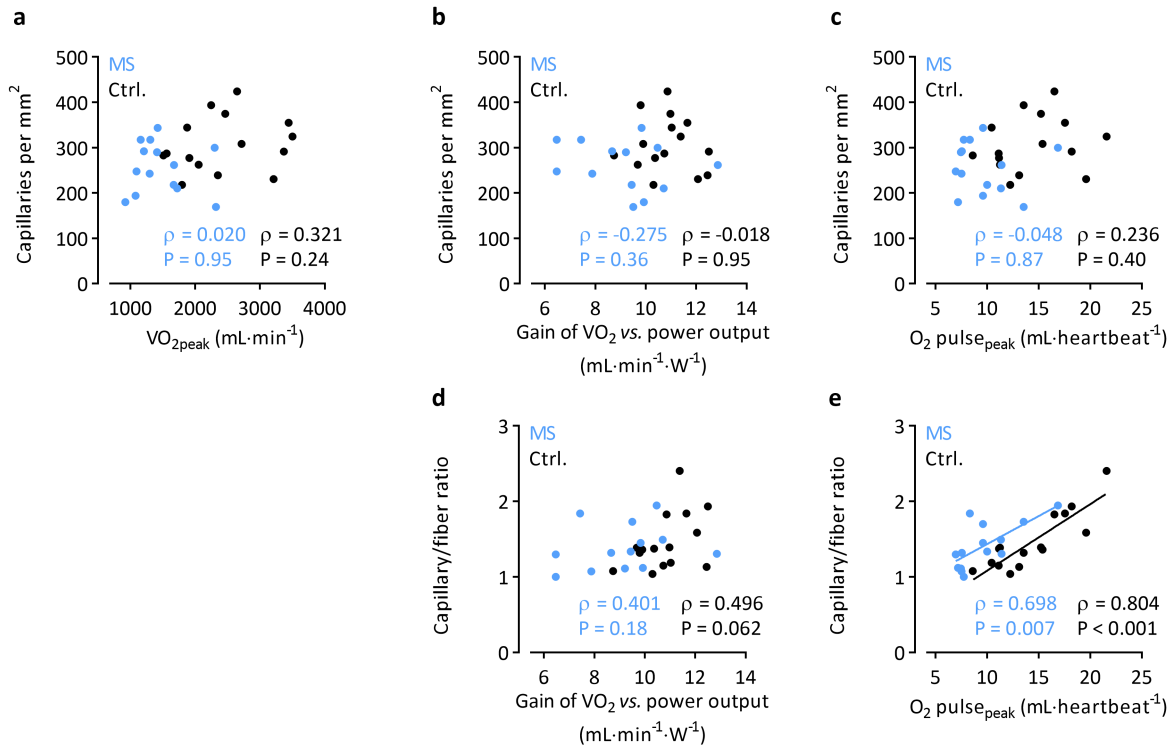
Supplementary Figure 1, related to Figure 2. Muscle fiber minimal Feret's diameter in biopsies from MS patients and healthy controls. Vastus lateralis biopsies were obtained from MS patients and healthy controls. Muscle fiber minimal Feret's diameter of type I, IIa and IIa/x fibers in MS and controls. ** P<0.01 for main effect of fiber type (from mixed model analysis).

Supplementary Figure 2, related to Figure 4. Muscle capillarity and cardiopulmonary exercise test variables. Vastus lateralis biopsies were obtained from MS patients and healthy controls to determine muscle capillarity by immunohistochemistry. Correlations are displayed between muscle capillary density and (a) peak oxygen uptake ($\dot{V}O_{2peak}$), (b) the gain of the relationship between $\dot{V}O_2$ vs. external power output, and (c) peak O_2 pulse ($O_2\ pulse_{peak}$). Figure panels (d-e) display the correlations between capillary/fiber ratio and (d) the gain of the relationship between $\dot{V}O_2$ vs. external power output, and (e) peak O_2 pulse ($O_2\ pulse_{peak}$). Note that the relation between capillary/fiber ratio and $\dot{V}O_{2peak}$ is shown in Figure 4d.

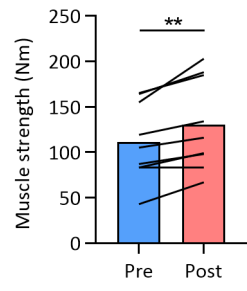
Supplementary Figure 3. Changes in muscle strength following exercise training in MS patients. Maximal isometric voluntary knee extensor strength before and after the exercise intervention in MS patients. ** P<0.01.



Supplementary Figure 1 , related to Figure 2.



Supplementary Figure 2, related to Figure 4.



Supplementary Figure 3.